SciEn

*Proceedings of 8th International Conference on Mechanical Engineering and Renewable Energy 2025*
*10-12 December, 2025, Chattogram, BANGLADESH*

SciEn Conference Series: Engineering Vol. 4, 2026, pp 123-128 https://doi.org/10.38032/scse.2026.4.62

# Biogenic Synthesis of Al-Mn doped ZnO nanoparticles: morphology, structure & photocatalytic activity

*Safat Anam[1,*], Israt Jahan Shammi[1] and Md. Masumul Haque[2]*

[1]Department of Chemical Engineering, Rajshahi University of Engineering & Technology, Rajshahi-6204, Bangladesh
[2]Department of Materials Science & Engineering, Rajshahi University of Engineering & Technology, Rajshahi-6204, Bangladesh

**ABSTRACT**

Green nanoparticles synthesis is gaining popularity for numerous applications. This study developed a safe, cost-effective, and ecologically sound process for producing pure and Al- Mn-doped ZnO nanoparticles from Phyllanthus Emblica (Amla) fruit extract using Zinc Nitrate as the precursor. A number of characterization techniques confirm the morphological and structural characteristics. Undoped and doped ZnO nanoparticles were developed without the rutile phase, according to XRD analysis. The SEM image showed that Al-Mn-doped ZnO nanoparticles were more agglomerated. 36.25 nm was the average size of pure ZnO NPs and it rises when doping level increases. The inclusion of Al and Mn into the ZnO lattice structure was verified via EDX analysis. UV-visible spectroscopy was used to evaluate the synthesized NPs' band gap energy and photocatalytic performance. Reduced band gap energy was revealed for 2% and 4% doped ZnO NPs. In addition, produced NPs had increased UV photocatalytic activity, especially for methylene blue degradation. The highest degradation rate was observed for 4% doping. This study found biosynthesized ZnO nanoparticles to be effective water purifiers.

Keywords: Green Synthesis, ZnO nanoparticles, Amla extract, Doping, Photocatalytic.



## 1. Introduction

At present, nanotechnology is regarded as a dependable and cutting-edge field because of the broad features of nanomaterials. The intriguing behaviors and features of metal or metal oxide nanoparticles have prompted substantial research into their properties such as electronic, magnetic, optical, antibacterial, and catalytic properties [1]. Various synthesis process including physical and chemical approaches has been explored. Green synthesis is a chemical synthesis method that uses plant-based chemicals like flavonoids, alkaloids, and phenolics to decrease metal ions and make nanoparticles [2]. This method is cheaper and better for the environment than traditional chemical methods [3]. ZnO is an inorganic semiconductor from the II-IV family. At ambient temperature, it possesses a wide BGE of about 3.37 eV and a BE of approximately 60 million eV [4]. ZnO nanoparticles may be able to make hydroxyl radicals and operate as photocatalyst since they are unique in form, size, and composition [5]. The biogenic production process is a cheaper way to get these specific features of ZnO. The synthesis of ZnO nanoparticles has been recorded utilizing diverse plant sources. For example, the leaves Ocimum tenuiflorum (Tulshi) [6], Azadirachta indica (Neem) [7], are used to make ZnO nanoparticles. Zinc oxide nanoparticles are derived from Mangifera indica (Mango) and Citrus sinensis (L.) Osbeck (Sweet orange) peels [8], Cicer arietinum (Chickpea) seeds [9], and Acanthophyllum laxiusculum roots [10]. Ahmad et al. (2022) used Prunus cerasifera to synthesize Ag doped ZnO nanoparticles via hydro-thermal route and exhibited efficient photocatalytic activity under solar light irradiance against bromocresol green and bromophenol blue [11]. Naiel et al. (2022) utilize sea lavender extract to synthesize ZnO NPs, which exhibited enhanced antioxidant and antibacterial capabilities [12].

This study utilizes Phyllanthus Emblica (Amla) fruit extract that reduces the NPs from the ZnO precursor. Although there have been several reported ways to synthesize ZnO, no one in the literature has made any claims about synthesizing ZnO-NPs with fruit extract from Amla. There are secondary metabolites in Amla extract that can reduce the nanoparticles from its precursors [13]. Amla is a sustainable and economically viable raw material for ZnO manufacture since it is abundant in Bangladesh. Several studies reported doping ZnO with impurity atoms to increase the photocatalytic activity. Doping introduces new energy levels within the band gap that inhibits electron-hole recombination under radiation, enhancing light absorption and charge separation [14]. When exposed to visible light, the transition metals manganese (Mn) and aluminum (Al) doped NPs gives improved photocatalytic degradation along with energy utilization. By adding aluminum to ZnO NPs, the electron capturing technique can improve electron-hole separation [15]. Doping with Mn also improves surface electron excitation and light absorption in the visible spectrum [16]. The photocatalytic stability and endurance of Al-Mn co-doped ZnO nanoparticles has not been extensively studied. In order to assess their environmental and economic potential for treating wastewater containing textile dyes, this study used an environmentally friendly method to create Al-

*Corresponding Author Email Address: safat.anam@che.ruet.ac.bd Published By: SciEn Publishing Group

Mn doped ZnO NPs by analyzing their morphological and structural properties and photodegradation performance using an extract from the Amla fruit.

## 2. Materials and methods

### 2.1 Materials

This investigation used chemicals of analytical grade. The main ingredients are: (1) Zinc Nitrate, $Zn(NO_3)_2.6H_2O$(ZnO precursor) from Researchlab- India (96.94%); (2) Aluminium Nitrate, $Al(NO_3)_3.9H_2O$ of (99%); and Manganese Sulphate, $MnSO_4.H_2O$ of (98.96%) as Al and Mn precursor; (3) Dry Amla fruit powder to extract reducing agent; (4) Distilled water, (5) Methylene Blue (MB).

### 2.2 Fruit Extract Preparation

The green Amla fruits were cleaned with purified water and then dried. After being chopped, 200 grams of Amla fruits were placed in a 60°C oven for an entire night before being crushed with a mortar. For almost four hours at 60°C, a magnetic stirrer blended 500 ml of heated deionized water with 30 grams of dried fruit powder. Filtration through whatman filter paper was performed once the mixture had come down to room temperature. In preparation for further testing, the collected extract was chilled to 14°C in the refrigerator.

### 2.3 Synthesis of Zinc Oxide Nanoparticles

Prior synthesis of ZnO NPs, 10 gram of Zinc nitrate salt precursor and 100 ml distilled water was mixed thoroughly. A 60 ml dropwise addition of Amla fruit extract was made. Using magnetic stirring at 200 rpm, the temperature was maintained at 60°C for four hours. To maintain a constant pH of 6.5, a few drops of sodium hydroxide were included into the mixture. The mixture hue resembled a blend of yellow and brown but the texture became thicker gradually. To prepare 2% and 4% in 1:1 ratio Al and Mn doped ZnO, 0.13 and 0.25 gm of $Al(NO_3)_3.9H_2O$ and 0.057 and 0.114 gm of $MnSO_4.H_2O$ are added to the solution respectively in this stage. After that, the solution was stored for 24 h to facilitate the gelation process. It took 20 minutes of centrifugation at 2500 rpm after cleaning to collect the gel. Ethanol and distilled water were used for the cleaning task. The flake-like particles were created by drying the collected soaked particles overnight in an oven set at 100 °C. To ensure even heating during calcination, the flakes were grinded before heated. The ground particles were calcined at 450°C in a muffle furnace for 4.5 hours. Resulting calcined powder was preserved for the photocatalytic test and characterization purposes.

### 2.4 Characterization of Synthesized NPs

The XRD analysis was carried out using a Shimadzu LabX XRD-6100 diffractometer in order to determine the NPs' crystallinity. SEM-EDS analysis revealed the morphology and structure of the NPs.. For the purpose of determining the BGE of the NPs, a Shimadzu UV-3600 Plus UV-Vis with NIR scanner was utilized.

### 2.5 Photocatalytic Activity Analysis

Degradation of MB dye in our synthesized ZnO NPs was examined for photocatalytic activity. A photoreactor equipped with a UV light source was chosen for this purpose. A concentration of 10 mg/L was achieved by dissolving the required quantity of dye in sterile water to create the MB solution. Half a milligram of ZnO catalyst was added to a beaker in a reaction vessel that held 30 mL of the stock MB solution. To create adsorption equilibrium, the mixture was stirred for 20 minutes set to 500 rpm using a magnetic stirrer within the photoreactor while being shielded from UV radiation. Following a designated duration of 15, 60, or 95 minutes, 5 mL of the mixture was removed from the beaker and subjected to filtration to eliminate the catalyst. The procedure was carried out after the reaction attained equilibrium and the UV light (24 watts) was activated. To observe the reaction, an UV-Vis spectrometer (200–800 nm) recorded the MB dye's peak absorption at regular intervals. The technique has been utilized on ZnO samples, encompassing both doped and undoped variations. The efficiency of degradation was determined by analyzing the concentrations of MB at different time.

## 3. Result and discussion

### 3.1 XRD Analysis

The micro-strain, crystalline structure, size, and crystalline phases of both undoped and doped ZnO NPs are assessed using XRD. Both the doped and undoped ZnO XRD spectra are displayed in the Figure 1. The undoped zinc oxide sample shows peaks at the 2θ angle in the XRD diagram. of 31.80°, 34.44°, 36.27°, 47.55°, 56.65°, 62.88°, 67.53°.Where peaks are being observed related to planes (101) which is predominant (002), (101), (102), (110), (103), (112) and matched with the International Centre for Diffraction Data reference code (01-076-0704) which confirm the tetragonal anatase phase of Zinc Oxide and characterized the sample as zinc oxide nanoparticles. Doped samples of zinc oxide have the same XRD pattern as undoped samples. It attests to the fact that doping had no effect on the zinc oxide's crystal phase. Furthermore, no additional peaks were seen in the XRD of the doped sample, indicating that the sample was free of contaminants such as oxides during production. The structural parameters for the undoped and doped ZnO samples are shown in Table 1. This study demonstrates that the size of the crystallites decreases as the doping percentage rises. A significant discovery is that, while size rises when doped compared to undoped, size falls again when doping concentrations rise. Variations in radius size may generate strain or tension, which in turn hinders grain growth. Dopant and host atoms exhibit differences in atomic size, valency, and electronegativity, which lead to dopants frequently acting as pins at grain boundaries, thereby restricting the mobility of these boundaries. As a consequence, as strain inside the crystal structure increases, the crystallites' sizes decrease.

### 3.1 SEM Analysis

The particle size and shape of pure and doped ZnO nanoparticles were studied using SEM analysis. Fig. 2 displays SEM micrographs of pure, 2%, and 4% doped ZnO at 100,000× magnifications. Particle size distribution was analyzed using ImageJ and Origin software. Undoped ZnO had almost spherical particles and an average particle size of 36.25 mm. Increased Al-Mn content in the doping compound causes ZnO to aggregate more than pure ZnO. As a result, particle size raised from 36.25 to 43.68 and 59.87 nm for 2% and 4% doped ZnO. Particle agglomeration may be linked to ionic radius. Al and Mn dissolved into ZnO host lattice by occupying $Zn^{2+}$ sites, expanding volume. Due of the negatively charged adsorbent surface at low pH, pH may also

contribute. They are more attracted to positively charge complex cations in solution when pH drops, increasing adsorption and agglomeration accelerates. Agglomeration is also affected by metal content, temperature, time, and others. Table 1 shows the structural properties of the synthesized nanoparticles.

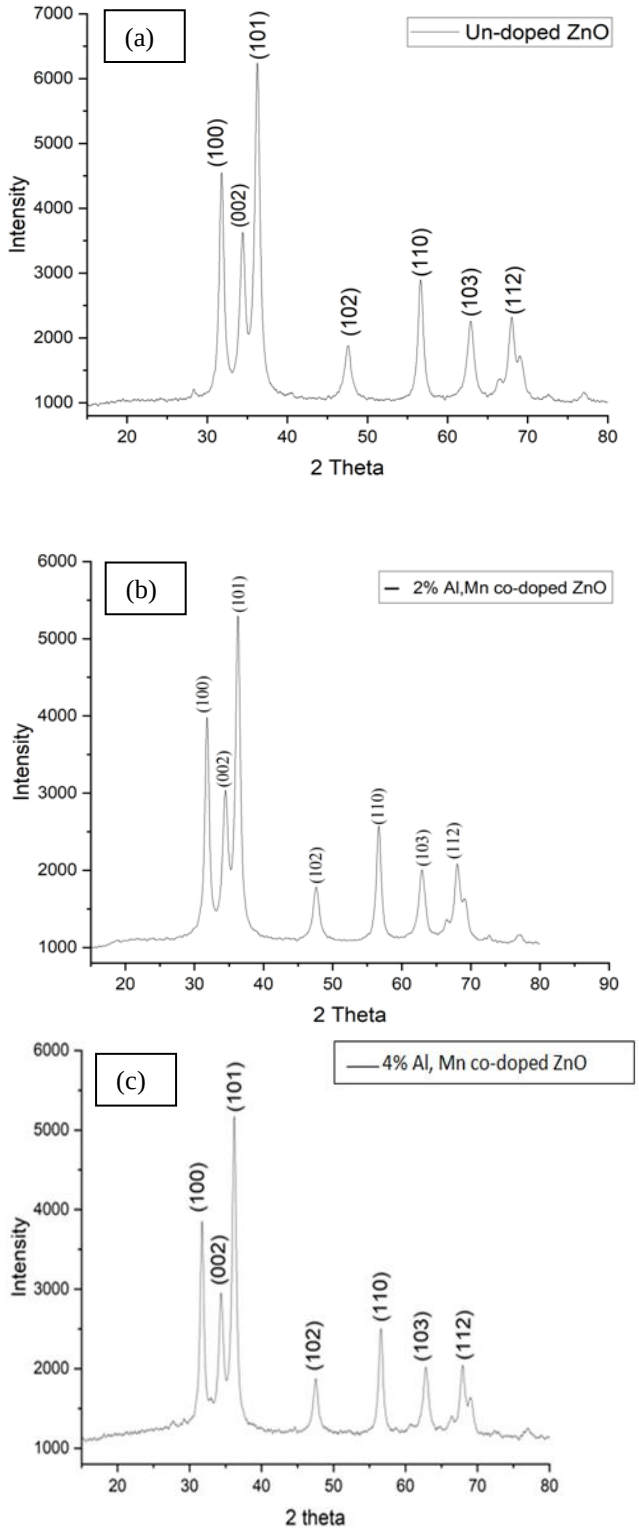


**Fig. 1** XRD result of (a) Pure, (b) 2% Al-Mn doped and (c) 4% Al-Mn doped ZnO.

3.3 EDS Analysis

EDS analysis serves to define the chemical composition of materials. It shows how much of each element is present in the pure and doped ZnO nanoparticles.

**Table 1** Key properties of the synthesized NPs

| Sample | Major peak (2θ) | Crystallinity (nm) | Micro Strain × $10^{-3}$ | Avg. Particle Size (nm) | Band Gap (eV) |
|---|---|---|---|---|---|
| Pure ZnO | 36.261 | 7.613 | 13.408 | 36.25 | 3.37 |
| 2% doped ZnO | 36.214 | 8.629 | 11.361 | 43.68 | 3.14 |
| 4% doped ZnO | 36.304 | 7.231 | 14.141 | 59.87 | 3.06 |

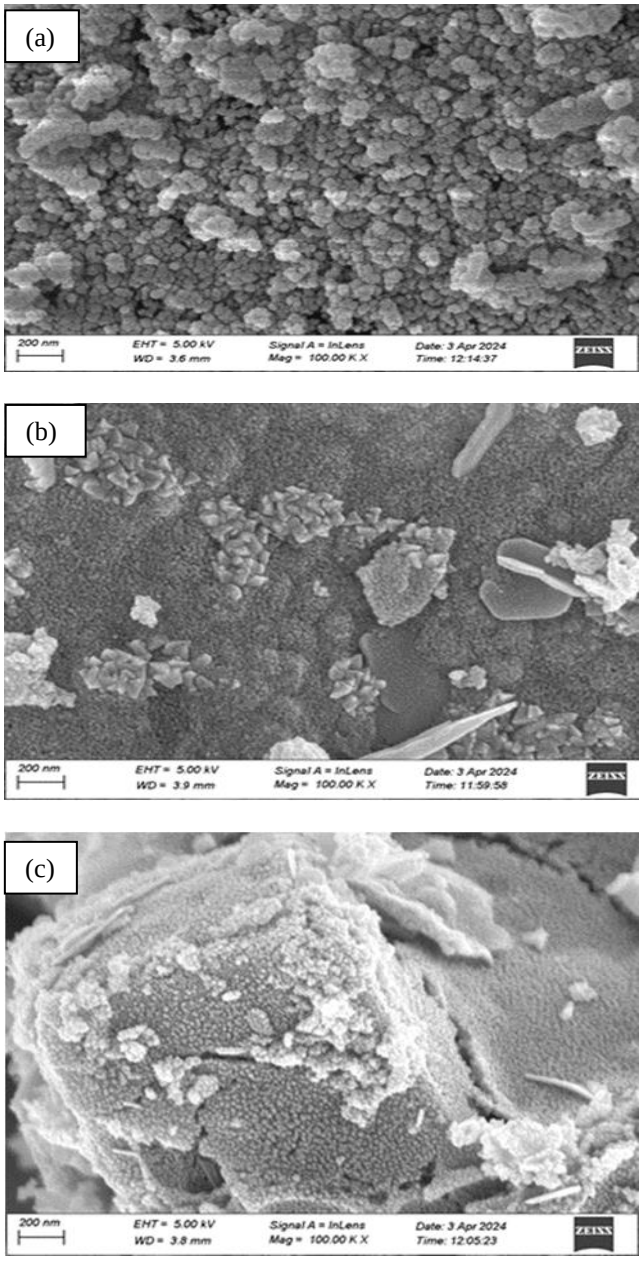


**Fig. 2** SEM image of (a) Pure, (b) 2% Al-Mn doped and (c) 4% Al-Mn doped ZnO.

Fig. 3 displays the EDS analysis result and confirms the purity of both doped and undoped ZnO nanoparticles. Fig. 3(b) and (c) demonstrate that ZnO nanoparticles include Al and Mn in varying ratios. The presence of contaminants in the samples is indicated by a few small peaks in the EDS spectra. One probable explanation for this could be that

organic residues were not completely removed during the calcination process. The phase purity was validated by XRD data, and the successful incorporation of doped elements into the host ZnO structure was confirmed by EDS results.
results.

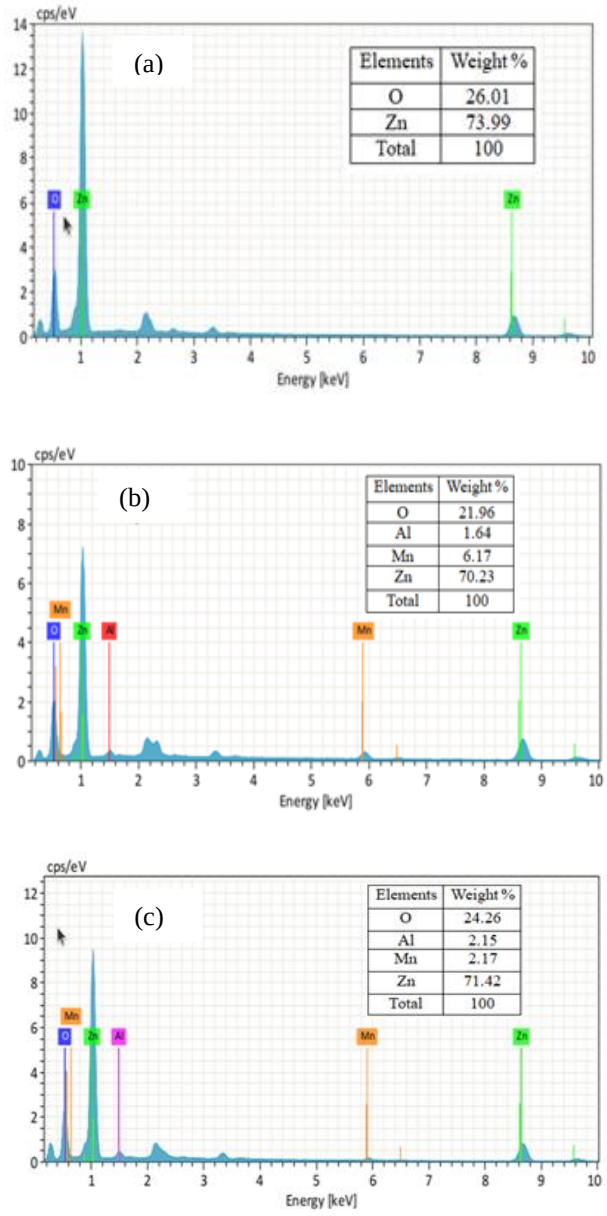


**Fig. 3** SEM image of (a) Pure, (b) 2% Al-Mn doped and (c) 4% Al-Mn doped ZnO.

3.4 UV-Visible Spectroscopy Analysis

At ambient temperature, the BGE of ZnO is around 3.37 eV. This was validated through the UV-Vis analysis presented in Fig. 4(a). Mn atoms have the ability to function as acceptor impurities when added to the ZnO lattice correspond to a narrowed band gap as localized states arise inside it explained by the charge exchange that occurs between the ZnO host lattice and the Mn ions. Al doping can have both donor and acceptor effects on the ZnO lattice, depending on the doping concentration and the growth conditions. Al can form Al-Zn complexes acting as acceptor centers and introducing localized states within the band gap, which can reduce the band gap energy. When ZnO is doped with 2% Al and Mn, its band gap energy (BGE) is reduced to approximately 3.14 electron volts (eV). Introduction of Al and Mn atoms into the ZnO lattice affects its electronic structure, leading to a reduced BGE compared to pure ZnO. Doping with 4% Al- Mn results in a BGE of nearly 3.06 eV.

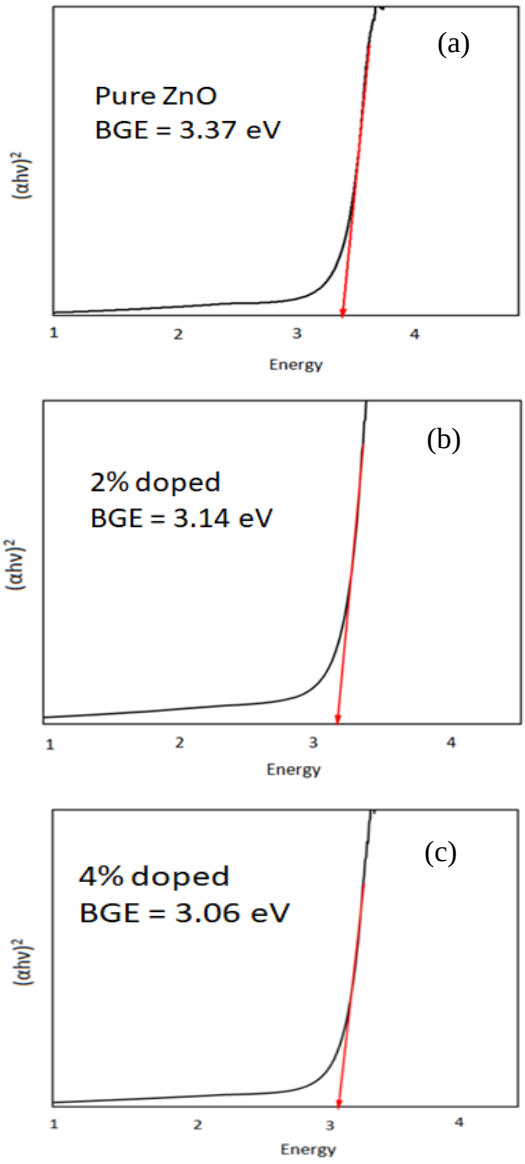


**Fig. 4** BGE of (a) Pure, (b) 2% Al-Mn doped and (c) 4% Al-Mn doped ZnO.

3.5 Photocatalytic Performance Analysis

The photocatalytic effectiveness of the synthesized NPs was examined against methylene blue dye. The absorbance of pure and Al-Mn doped ZnO samples were analyzed at various time intervals. The UV-Vis spectrum of MB dye pollutant under doped and undoped ZnO is shown in Fig. 5. Again, Fig. 6 shows the photodegradation of MB dye when exposed to UV radiation. The absence of light did not change MB concentration, indicating that MB solutions were stable. A decrease in concentration with the addition of catalysts and UV light indicates that photocatalysis is responsible for the reduction of methylene blue. The breakdown of MB is reflected by the decrease in absorbance over time.
Undoped ZnO degraded 26.90% after 15 min and 83.25 % after 95 min. In addition, ZnO nanoparticles doped with 2% and 4% Al-Mn demonstrate remarkable efficacy in degrading MB. The photocatalytic efficiency raised from 31.7 % to 87.71 % for 2% Al-Mn doping and 49.9% to 90.10% for 4% doping.

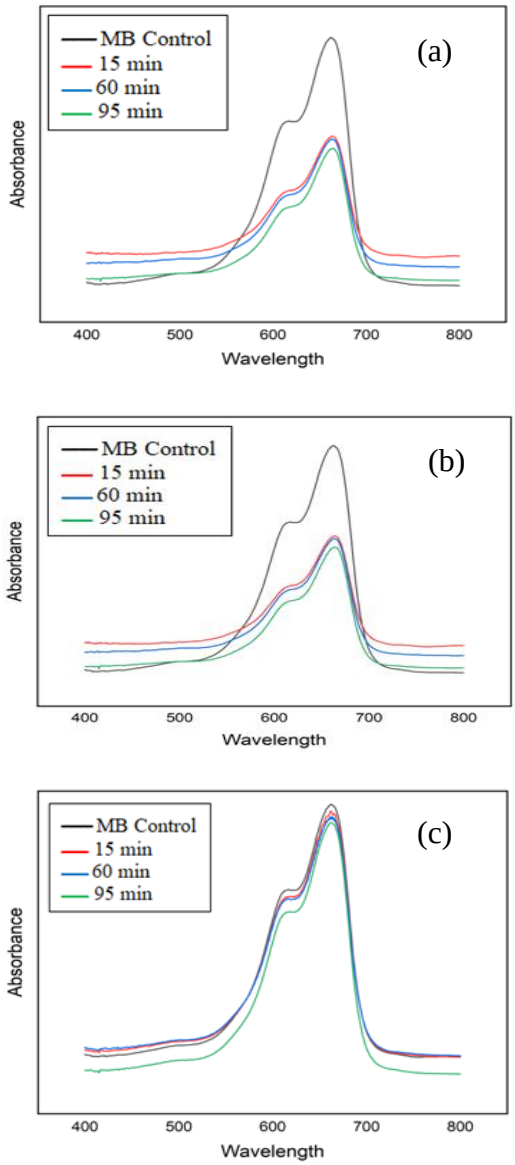


**Fig. 5** Absorption spectra of (a) Pure, (b) 2% Al-Mn doped and (c) 4% Al-Mn doped ZnO.

The photodegradation efficiency is calculated by the following equation:

$$\text{Efficiency} = (1 - A_t/A_0) \times 100\% \quad (1)$$

After 95 minutes of irradiation, the ZnO doped with 4% Al-Mn achieves the maximum degrading efficiency.

**Table 2** Photodegradation performance of undoped and doped ZnO under UV light.

| Sample | Concentration (after 15 min) | % Degradation (15 min) | Concentration (after 95 min) | % Degradation (95 min) | Avg. Degradation Rate ($min^{-1}$) |
|---|---|---|---|---|---|
| Pure ZnO | 0.73 | 26.9 | 0.16 | 83.25 | 0.00225 |
| 2% doped | 0.68 | 31.7 | 0.12 | 87.71 | 0.00307 |
| 4% doped | 0.50 | 49.9 | 0.09 | 90.10 | 0.00339 |

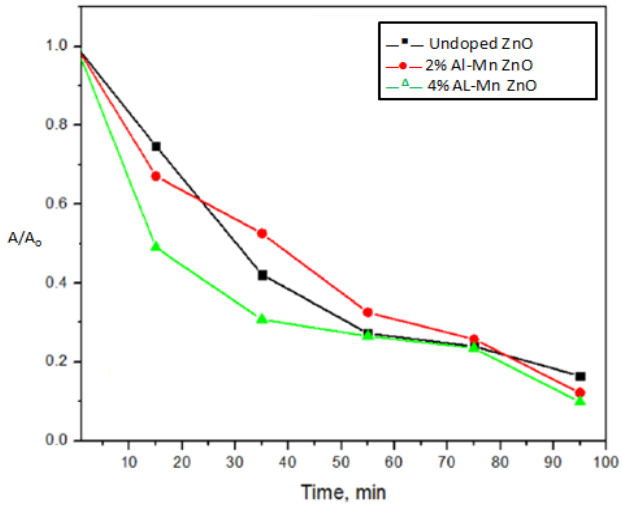


**Fig. 6** Variation of MB concentration with time.

## 4. Conclusion

This study introduces an innovative biogenic method for integrating Amla fruit extract into the synthesis of undoped and Al-Mn doped ZnO nanoparticles, along with their application in photocatalytic processes. XRD analysis confirmed that the anatase phase remained unchanged when changing the doping concentration, although a significant effect was observed for crystallite size and microstrain. Results from SEM analysis confirmed that particle size varied with doping concentration and that aggregate formation was affected by time, temperature, pH, and doping concentration. Phase purity and presence of $Zn^{2+}$, $Al^{3+}$ and $Mn^{2+}$ ions in doped ZnO nanoparticles were verified by EDX data. A downward fall was demonstrated for the band gap with increasing concentration of doping (3.14 eV for 2% and 3.06 for 4%) from UV-Vis analysis. Improved degradation efficiency was seen in 4% Al-Mn doped ZnO with the most outstanding performance (90.10%). The results show that Al-Mn doped ZnO is very useful for removing dyes and purifying water.

## 5. References

[1] K. Parveen, V. Banse, and L. Ledwani, "Green synthesis of nanoparticles: Their advantages and disadvantages," in *AIP conference proceedings*, 2016, vol. 1724, no. 1: AIP Publishing LLC, p. 020048.

[2] S. Hasan, "A review on nanoparticles: their synthesis and types," *Res. J. Recent Sci,* vol. 2277, p. 2502, 2015.

[3] H. A. Salam, P. Rajiv, M. Kamaraj, P. Jagadeeswaran, S. Gunalan, and R. Sivaraj, "Plants: green route for nanoparticle synthesis," *Int Res J Biol Sci,* vol. 1, no. 5, pp. 85-90, 2012.

[4] P. J. P. Espitia, N. d. F. F. Soares, J. S. d. R. Coimbra, N. J. de Andrade, R. S. Cruz, and E. A. A. Medeiros, "Zinc oxide nanoparticles: synthesis, antimicrobial activity and food packaging applications," *Food and bioprocess technology,* vol. 5, no. 5, pp. 1447-1464, 2012.

[5] L.-E. Shi, Z.-H. Li, W. Zheng, Y.-F. Zhao, Y.-F. Jin, and Z.-X. Tang, "Synthesis, antibacterial activity, antibacterial mechanism and food applications of ZnO nanoparticles: a review," *Food Additives & Contaminants: Part A,* vol. 31, no. 2, pp. 173-186,

2014.

[6] A. Shahzaib, N. Nishat, S. M. Alshehri, T. Ahamad, and Z. Haque, "Biogenically fabricated Tulsi-infused ZnO–CuO nanocomposites for enhanced dye reduction and adsorption," *Hybrid Advances,* vol. 5, p. 100145, 2024.

[7] L. Yadeta Gemachu and A. Lealem Birhanu, "Green synthesis of ZnO, CuO and NiO nanoparticles using Neem leaf extract and comparing their photocatalytic activity under solar irradiation," *Green Chemistry Letters and Reviews,* vol. 17, no. 1, p. 2293841, 2024.

[8] N. A. N. Mohamad, N. A. Arham, J. Jai, and A. Hadi, "Plant extract as reducing agent in synthesis of metallic nanoparticles: a review," *Advanced Materials Research,* vol. 832, pp. 350-355, 2014.

[9] I. Das and D. Borah, "Microbial biosurfactant-mediated green synthesis of zinc oxide nanoparticles (ZnO NPs) and exploring their role in enhancing chickpea and rice seed germination," *Discover Nano,* vol. 19, no. 1, p. 174, 2024.

[10] Z. Madadi and T. Bagheri Lotfabad, "Aqueous extract of acanthophyllum laxiusculum roots as a renewable resource for green synthesis of nano-sized titanium dioxide using sol-gel method," *Advanced Ceramics Progress,* vol. 2, no. 1, pp. 26-31, 2016.

[11] S. B. Jaffri and K. S. Ahmad, "Foliar-mediated Ag: ZnO nanophotocatalysts: green synthesis, characterization, pollutants degradation, and in vitro biocidal activity," *Green Processing and Synthesis,* vol. 8, no. 1, pp. 172-182, 2019.

[12] B. Naiel, M. Fawzy, M. W. A. Halmy, and A. E. D. Mahmoud, "Green synthesis of zinc oxide nanoparticles using Sea Lavender (Limonium pruinosum L. Chaz.) extract: characterization, evaluation of anti-skin cancer, antimicrobial and antioxidant potentials," *Scientific Reports,* vol. 12, no. 1, p. 20370, 2022.

[13] I. Ashraf, N. Singh, and A. Agarwal, "Green synthesis of iron oxide nanoparticles using Amla seed for methylene blue dye removal from water," *Materials Today: Proceedings,* vol. 72, pp. 311-316, 2023.

[14] Y. Zhu and Y. Zhou, "Preparation of pure ZnO nanoparticles by a simple solid-state reaction method," *Applied Physics A,* vol. 92, no. 2, pp. 275-278, 2008.

[15] F. Maldonado and A. Stashans, "Al-doped ZnO: Electronic, electrical and structural properties," *Journal of Physics and Chemistry of Solids,* vol. 71, no. 5, pp. 784-787, 2010.

[16] T. Fukumura *et al.*, "Magnetic properties of Mn-doped ZnO," *Applied Physics Letters,* vol. 78, no. 7, pp. 958-960, 2001.

## 6. NOMENCLATURE

| *Symbol* | *Meaning* | *Unit* |
|---|---|---|
| *NPs* | Nanoparticles | - |
| *BGE* | Band gap energy | (eV) |
| *BE* | Binding Energy | meV |
| $\theta$ | diffraction angle | (radian) |
| $A_0$ | Initial dye conce. | mg/L |
| $A_t$ | Dye conc. at time t | mg/L |